



The Electronic Properties of the Silver Clusters in Gas Phase and Water

Mariana Virginia Popa

Electronic and Telecommunication, Autonomous University of the Hidalgo State, Mexico

Email address:

virginia_popa@yahoo.com.mx, pmarianavirginia@yahoo.com

To cite this article:

Mariana Virginia Popa. The Electronic Properties of the Silver Clusters in Gas Phase and Water. *International Journal of Computational and Theoretical Chemistry*. Special Issue: Electronic Proprieties in Computational Chemistry. Vol. 3, No. 3-1, 2015, pp. 36-57.

doi: 10.11648/j.ijctc.s.2015030301.13

Abstract: En this article are presented the theories work for clarify the structure of all silver cluster in gas phase and water and are compared the results with experimental data for see which levels of theory describe better the propriety of the silver cluster. Are calculated different value of the bond, ionization potentials and frequencies, electron affinities and binding energy method employed ab initio and relativistic bases. Are optimization with the following levels of theories: HF/LANL1MB, HF/LANL2MB, HF/LANL2DZ, B3LYP/LANL1MB, B3LYP/LANL2MB, B3LYP/LANL2DZ, MP2/LANL2DZ, DFT/PBE/SDD and DFT/PBE/3-21G**.

Keywords: Silver, Relativistic Effects, Metal Clusters, Silver Cluster in Water

1. Introduction

In the past two decade has been showing great interest for explanation the electronics proprieties of silver cluster with the nanometre dimension due to the proprieties who to exhibit the cluster generally, are different of the solid state [1,2,3] and molecular [4].

The study of the structure of the clusters of dimension nano to require to compare the date of the different experiments and theories.

The extraordinary proprieties of silver clusters to give a reason a much investigator to realize the works in photography, catalysis and new materials of electronic [5, 6-14].

Has been moderate that the relativistic effects influence in the electronic proprieties, so how in the geometry of the metals of transition so that gold, copper and silver [15]. The orbital 6s in gold to contract for the relativistic effect [15].

In [16] has been made the study with ion of silver with spectroscopy of mass. The neutral clusters has been obtained bombardment sheet of metal with ion Xe. Has been regard who the distribution of mass similar for negative and positive clusters. Has been analyze the structure of anion cluster $Ag_n(n=1-9)$ useful the electronic spectroscopy with gas He [17]. With nuclear magnetic spectroscopy of resonance and ultraviolet absorption spectroscopy has been

evidence the Jahn-Teller effect for Ag_3 [18,19]. Has been employed optic spectroscopy in the Ar matrix to characterize Ag_4 and has been evidence two isomeric states D_{2h} and C_{2v} with the difference between isomeric of 0.2 eV [20]. Employed the electronic spin resonance has been evidence the dimer, trimer and pentamer with the Jahn-Teller effect for the silver clusters [21, 22].

With the generator of N_2 laser, the vertical ionization potentials for $Ag_n (n < 100)$ has been study [23,24].

The photoelectron spectroscopy [25, 26] is a powerful technique for to study of electronic structure of metallic clusters and a very good method for adiabatic electronic affinity. The anionic clusters are separated with a mass spectrometer.

Has been evidence the alternate of the values for vertical electronic affinity with the variation even/odd (until 40 atoms) of silver used the photoelectron spectra in UV with He gas and laser with energy of the photon 6.4 y 7.9 eV [27, 28].

The frequency of the 2B_2 and 2A_1 has been evidence employed the optic spectra emission with Ag_3 evaporation at low pressure in He (100Torr) [29].

With the photoelectron spectra has been evidence the frequencies of the silver cluster ≤ 70 atoms [30]. Employed the optic resonance absorption for Ag_4^+ has been evidence the photofragmentation of anion cluster [31].

In the literature to attain various works with Ag clusters [32, 40].

In the experimental review silver clusters were prepared in an argon matrix by using high-temperature matrix preparation, [70].

In [71] silver ions are sputtered from a silver target using an intense and high-energy xenon-ion beam typically 10 mA, 24 keV. A development of the finite difference method is used to compute atomic-cluster absorption spectra. The spectra is compared with recent high-precision measurements of the X-ray mass absorption coefficient of silver in the X-ray absorption fine structure region, [72].

The degeneracy of the ground electronic state can lead to Jahn-Teller distortion along the e' bending coordinate. This lowers the symmetry from D_{3h} , to C_{2v} and correspondingly, the ${}^2E'$ state is resolved into 2B_2 (obtuse isosceles triangle) and 2A_1 (acute isosceles triangle) states.

The three 2B_2 extrema are equivalent global minima or saddle points in the ground state potential surface while the three equivalent 2A_1 extrema are saddle points or minima along the pseudorotation path. The D_{3h} equilateral triangle geometry occurs at a cusp on the surface.

The optical-absorption spectra of small mass-selected AgN clusters ($N=2-21$) embedded in solid argon are measured in the energy range 2.5-6.2 eV. Investigation of a continuous range of cluster sizes reveals the size development of the photoabsorption behavior, [73]. Briefly, silver ions are sputtered from a metal target using an intense, high-energy (typically 7 mA, 23KeV) xenon-ion beam, [73]. The photoionization mass spectrum obtained and vertical ionization potentials plotted in [74]. Photoelectron spectra of Ag_n^- clusters with $n = 1 - 21$ recorded at different photon energies ($h\nu = 54.025, 4.66, 5.0,$ and 6.424 eV) are presented in [75].

In [76] are investigated mass distributions of negative cluster ions of copper (Cu_n^-), silver (Ag_n^-), and gold (Au_n^-), obtained by the bombardment of metal sheets with Xe ions were investigated up to cluster size $n = 250$ and were compared with those of the positive cluster ions.

A continuous flow cryostat was used for these experiments. Temperatures above 3.5 K could be adjusted continuously and were measured using a calibrated carbon resistor and a vapour pressure thermometer, [77]. The reference [78] are employed photoelectron spectroscopy for negative ion Cu_n^- , Ag_n^- ($n = 1-10$), and Au_n^- ($n = 1-5$) are presented for electron binding energies up to 3.35 eV at an instrumental resolution

of 6-9 meV. The metal cluster anions are prepared in a flowing ion source with a cold cathode dc discharge.

Stable nanoparticle colloids of silver were obtained by irradiation of aqueous-alcoholic solutions of $AgNO_3$ in the presence of mesoporous SiO_2 powder and films modified with benzophenone (BP/ SiO_2), [79].

2. Results and Discussion

To introduce the electronic effects of correlation with B3LYP and B3PW91 functionals and relativistic effect with LANL2DZ and LANL2MB bases for Ag_2 are report the studys in reference [36], with BPW91 and SVWN IIa LANL2DZ base, the mistake for geometry are 3-4% y for frecuencies 6-8%. Also are reach the difference of the proprieties of Ag_2 above mencionen, with MP2 and S-VWN+Beke-Perdew functionals [37]. To be able that Ag_2 the distances are satisfy compared with 2.53 Å experimental data.

Fort the three atoms clusters has been realice divers study for top put in evidence the Jahn-Teller efecto and to calculation the electronics affinity [41-43]. Employed CC has been reported the date for silver clusters with 4,5 and 6 atoms [44].

3. Distance in Clusters

3.1. Neutral Dimers, Anions and Cations

How are to observe in the Fig. 1 (1a) [80], the distance for neutral cluster of two atoms obtained with HF/LANL1MB is the 2.91 Å. Employed the HF/LANL2MB method the distance are to contract 0.1 Å, see Fig. 2 (1a) [80]. With HF/LANL2DZ method has been obtained 2.73 Å for the neutral cluster with two atoms, see Fig. 3 (1a) [80], less who in the two events up mentioned. The difference of 0.18 Å between the cluster optimized with LANL2DZ and LANL1MB, who introduce the relativistic effects are possible for the 19 electrons in the valence layer employed LANLEDZ base, compared with 11 electrons introduced with LANL1MB base and the primitive employed [45, 46].

Not with standing this values are distant of the experimental data 2.5303(2) Å, see 39].

The dimer structure optimized are to present in the Figure of 1 at 9. The distance are in Å.

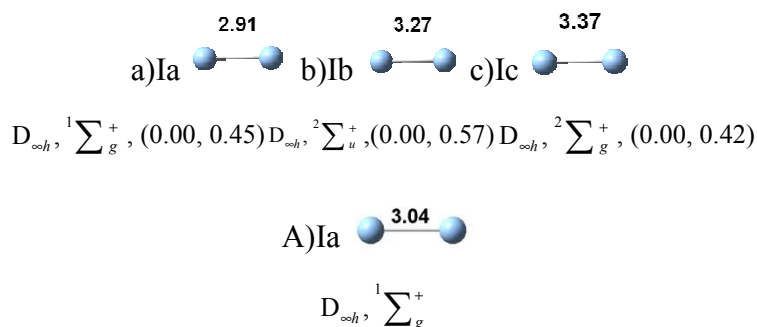


Fig. 1. The structure of dimer clusters with HF/LANL1MB: a) neutral; b) anions; c) cations. Between parenthesis are reported the relative energy, ΔE , (eV), and binding energy for atom (eV). A) for neutral in water.

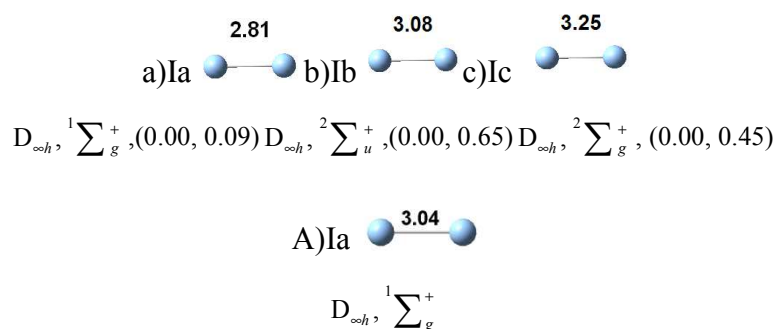


Fig. 2. The structure of dimer clusters with HF/LANL2MB: a) neutral; b) anions; c) cations. Between parenthesis are reported the relative energy, ΔE , (eV), and binding energy for atom (eV). A) for neutral in water.

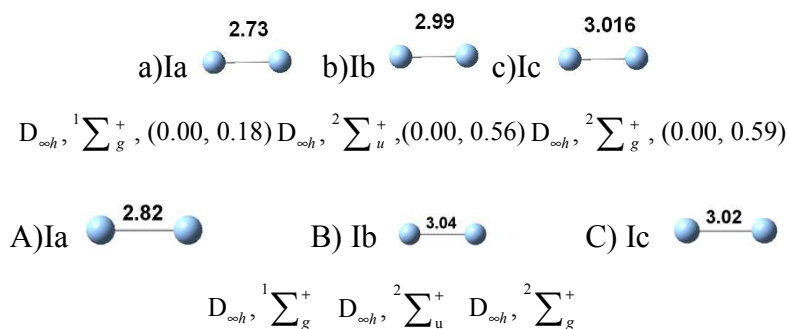


Fig. 3. The structure of dimer clusters with HF/LANL2DZ: a) neutral; b) anions; c) cations. Between parenthesis are reported the relative energy, ΔE , (eV), and binding energy for atom (eV). A, B) and C) for neutral anions, cations in water.

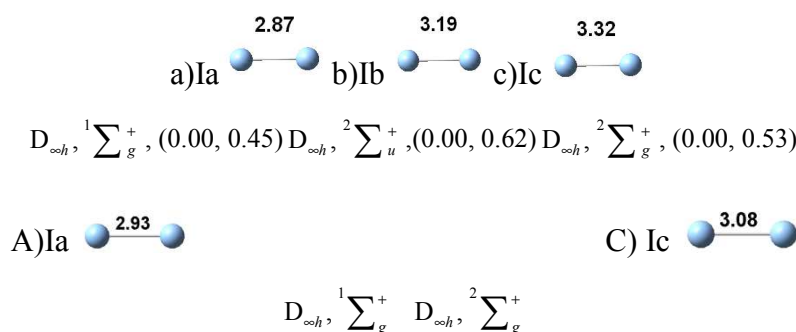


Fig. 4. The structure of dimer clusters with B3LYP/LANL1MB: a) neutral; b) anions; c) cations. Between parenthesis are reported the relative energy, ΔE , (eV), and binding energy for atom (eV). A, B) and C) for neutral anions, cations in water.

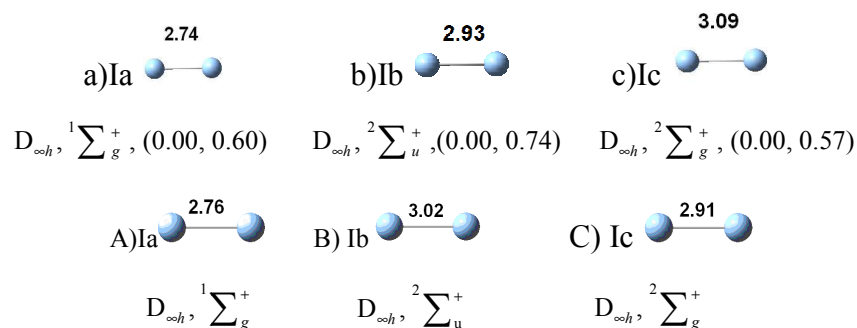


Fig. 5. The structure of dimer clusters with B3LYP/LANL2MB: a) neutral; b) anions; c) cations. Between parenthesis are reported the relative energy, ΔE , (eV), and binding energy for atom (eV). A, B) and C) for neutral anions, cations in water.

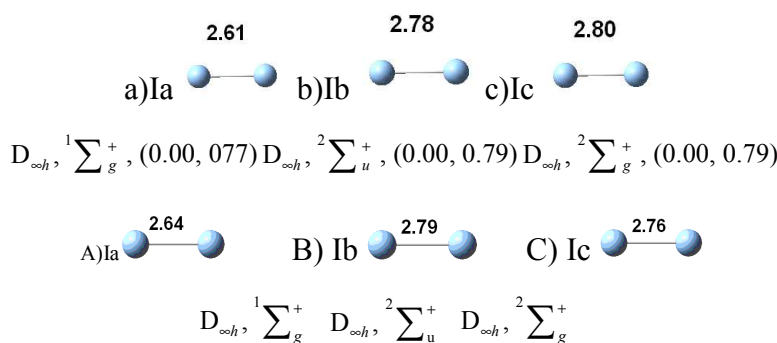


Fig. 6. The structure of dimer clusters with B3LYP/LANL2DZ: a) neutral; b) anions; c) cations. Between parenthesis are reported the relative energy, ΔE , (eV), and binding energy for atom (eV). A), B) and C) for neutral anions, cations in water.

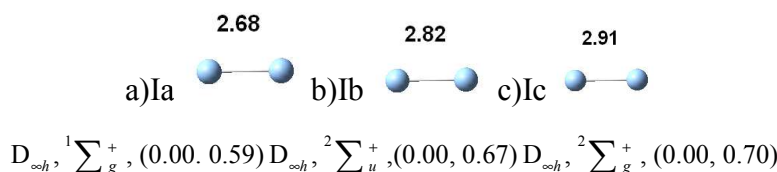


Fig. 7. The structure of dimer clusters with MP2/LANL2DZ: a) neutral; b) anions; c) cations. Between parenthesis are reported the relative energy, ΔE , (eV), and binding energy for atom (eV).

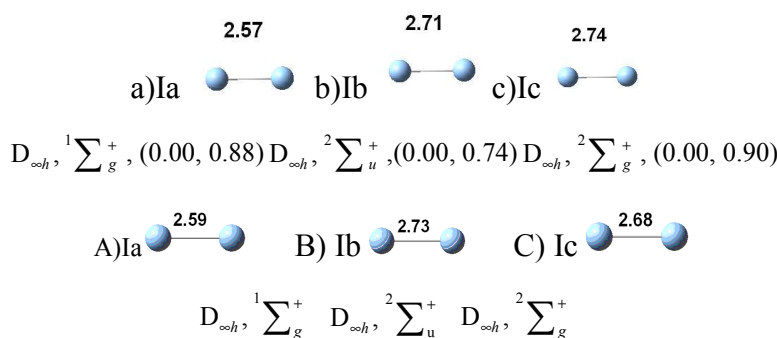


Fig. 8. The structure of dimer clusters with PBE/SDD: a) neutral; b) anions; c) cations. Between parenthesis are reported the relative energy, ΔE , (eV), and binding energy for atom (eV). A), B) and C) for neutral anions, cations in water.

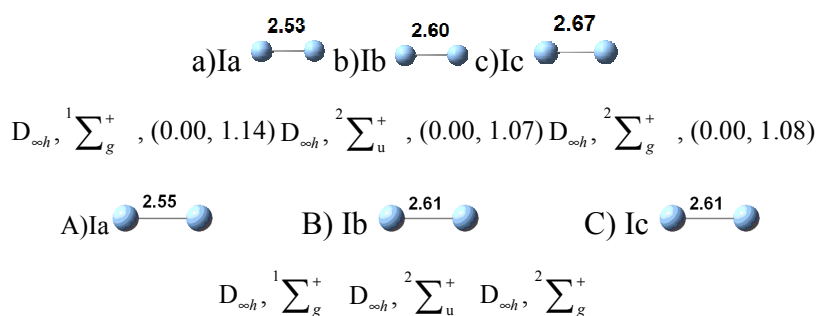


Fig. 9. The structure of dimer clusters with PBE/3-21G**: a) neutral; b) anions; c) cations. Between parenthesis are reported the relative energy, ΔE , (eV), and binding energy for atom (eV). A), B) and C) for neutral anions, cations in water.

For the dimer anion and cation calculated with HF/LANL1MB has been obtained 3.27 Å y 3.37 Å, see Fig. 1 (Ib y Ic); the cation cluster to designa an greater distance beteen of the atoms who anion, for the repulsion beteen the nucleos.

The distance beteen the atoms for anion cluster is greater who neutral cluster for the *core* electrons. Of this manner the electrons of the valence mantle make larger electronic

density. Employed DFT with B3LYP the distance beteen the atoms in neutral cluster lower in the following order LANL1MB > LANL2MB > LANL2DZ, see Fig.4 (Ia), Fig. 5 (Ia) y Fig. 6 (Ia). The 2.61 Å obtained with the DFT/B3LYP/LANL2DZ level is equal who reported in [47] but greater who employed B3P86/LANL2DZ (2.576 Å) and B3PW91/LANL2DZ (2.589 Å) [48]. With SVWN (LSDA)/LANL2DZ and SVWN5/LANL2DZ has been

obtained 2.501 y 2.508 Å [48], underestimate with experimental data 2.5303(2) Å [49]. For the neutral cluster of two atoms to employed MP2/LANLEDZ, are obtained 2.68 Å identically with [39] and with difference of 0.01 Å obtained with CCSD [39]. In water are obtained different value when are possible the ionization of anion, cation silver cluster.

For the anion and cation dimer, with the same level, has been obtained 2.91 Å y 2.82 Å, similar in the [39].

The value obtained for Ag_2 employed PBE/SDD is greater who 0.04 Å of the experimental value and minor with 0.04 Å who obtained with B3LYP/LANL2DZ and 0.01 Å that the value obtained with G96LYP/SDD [39]. In water, with DFT/PBE/3-21G** level are obtained 2.531 Å similar with the experimental data [49].

For the two atoms for anion with the DFT/PBE/3-21G** level has been attained 2.60 Å very near of the experimental data 2.62 Å [50].

For geometrically to describe the silver dimer cluster I employed PBE and 3-21G**.

3.2. Neutral Trimer, Anions and Cations

For the trimer are not experimental data above the distance of the atoms in clusters, for this reason I present the smallest and saddle point in the potential energy surface

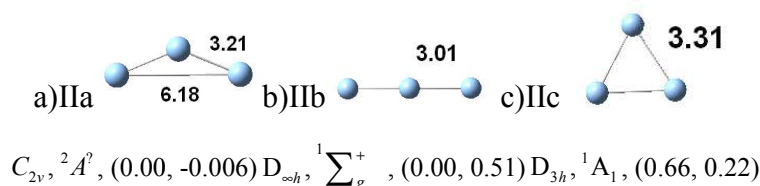


Fig. 10. The structure of trimer clusters with HF/LANL1MB: a) neutral; b) anions; c) cations. Between parenthesis are reported the relative energy, ΔE , (eV), and binding energy for atom (eV)

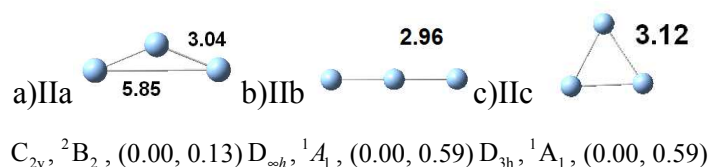


Fig. 11. The structure of trimer clusters with HF/LANL2MB: a) neutral; b) anions; c) cations. Between parenthesis are reported the relative energy, ΔE , (eV), and binding energy for atom (eV)

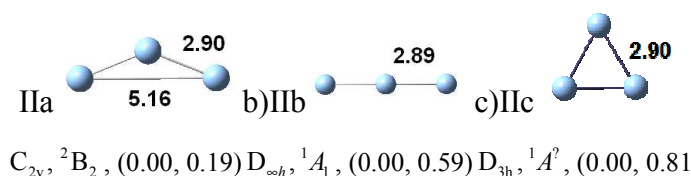
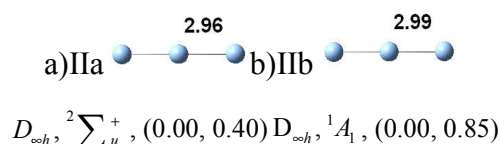


Fig. 12. The structure of trimer clusters with HF/LANL2DZ: a) neutral; b) anions; c) cations. Between parenthesis are reported the relative energy, ΔE , (eV), and binding energy for atom (eV)



for neutral clusters, with B3LYP and LANL1MB, LANL2MB y LANL2DZ bases, with MP2, and DFT/PBE/SDD y DFT/PBE/3-21G**.

Experimentally, [37, 41, 42, 51-55], and employed the theoretic jobs [32, 44, 56, 57] has been see the Jahn-Teller effects, more for the D_{3h} structure and are separate in smart, optuse triangle and to draw lines structure [25].

In ${}^2E'$ the electronic configuration is $(a_1')^2(e')^1$ where a_1' are the combination of three sAOs and e' is the orbital of the not connection double binding [57].

The 2B_2 is always more low in energie that 2A_1 , already who the apex atoms mix the caracter of the p orbital and the bonding augmented [58]. The autors of the [19] and [40], employed ab initio has been obtained who $(\sigma_g)^2(\sigma_u)^1$ is less estable with 0.05 eV who ${}^2E'$. The molecular orbitals $\sigma_g, \sigma_u, 2\sigma_g$ and as combination of 3 orbitals s of Ag_3 are the biding, not biding and antibiding, respectively [17].

For the structure trimer neutral the bonding has been obtained with MP2/LANL2DZ, see Fig. 16, and are equal with reported in [39].

The optimized structure are pictored in the following figure, when the biding are in Å.

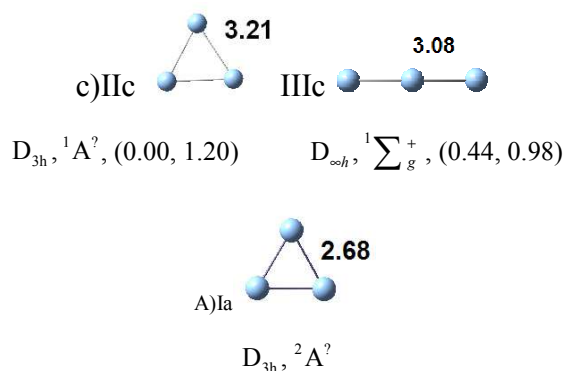


Fig. 13. The structure of trimer clusters with B3LYP/LANL1MB: a) neutral; b) anions; c) cations. Between parenthesis are reported the relative energy, ΔE , (eV), and binding energy for atom (eV). A) neutral in water.

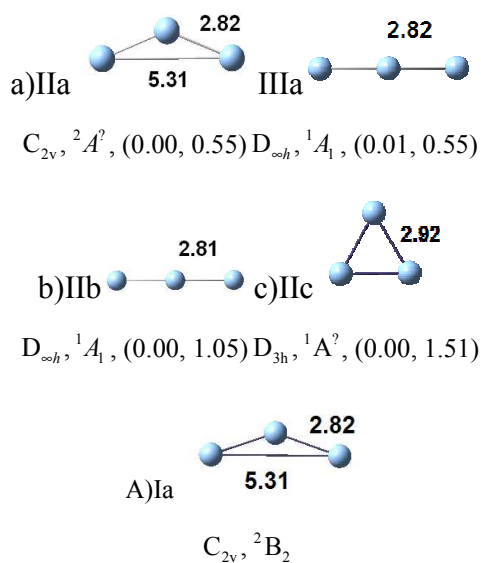


Fig. 14. The structure of trimer clusters with B3LYP/LANL2MB: a) neutral; b) anions; c) cations. Between parenthesis are reported the relative energy, ΔE , (eV), and binding energy for atom (eV). A) neutral in water

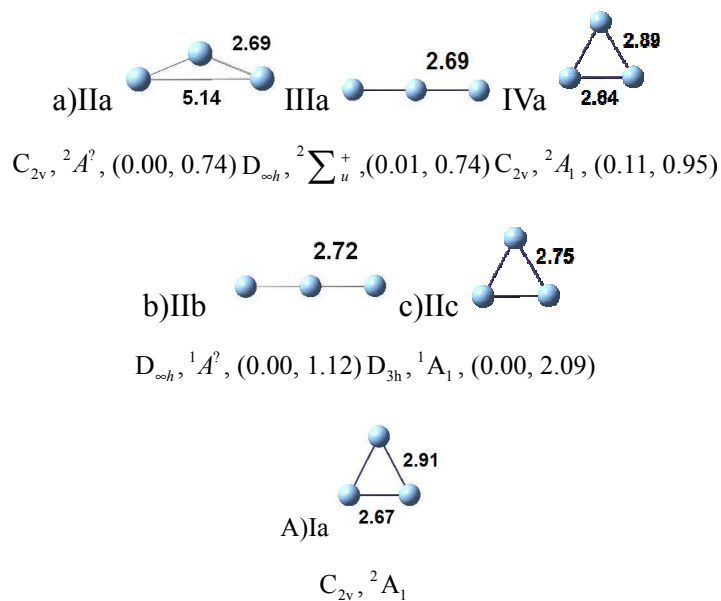


Fig. 15. The structure of trimer clusters with B3LYP/LANL2DZ: a) neutral; b) anions; c) cations. Between parenthesis are reported the relative energy, ΔE , (eV), and binding energy for atom (eV). A) neutral in water

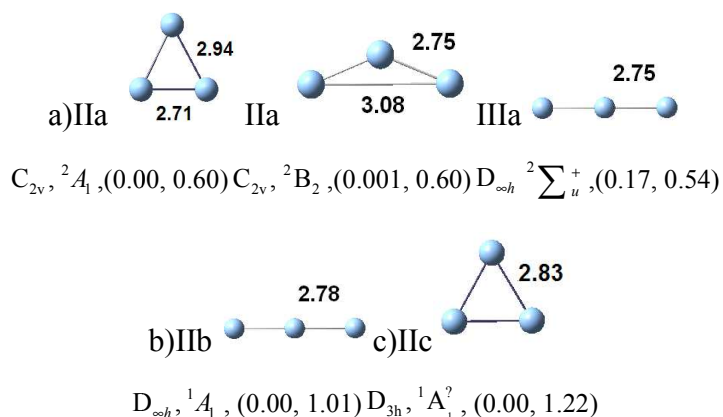


Fig. 16. The structure of trimer clusters with MP2/LANL2DZ: a) neutral; b) anions; c) cations. Between parenthesis are reported the relative energy, ΔE , (eV), and binding energy for atom (eV)

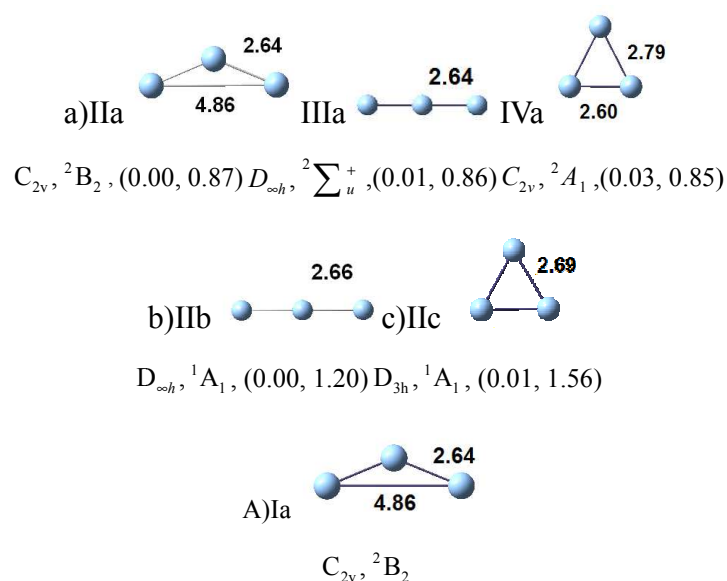


Fig. 17. The structure of trimer clusters with PBE/SDD: a) neutral; b) anions; c) cations. Between parenthesis are reported the relative energy, ΔE , (eV), and binding energy for atom (eV)

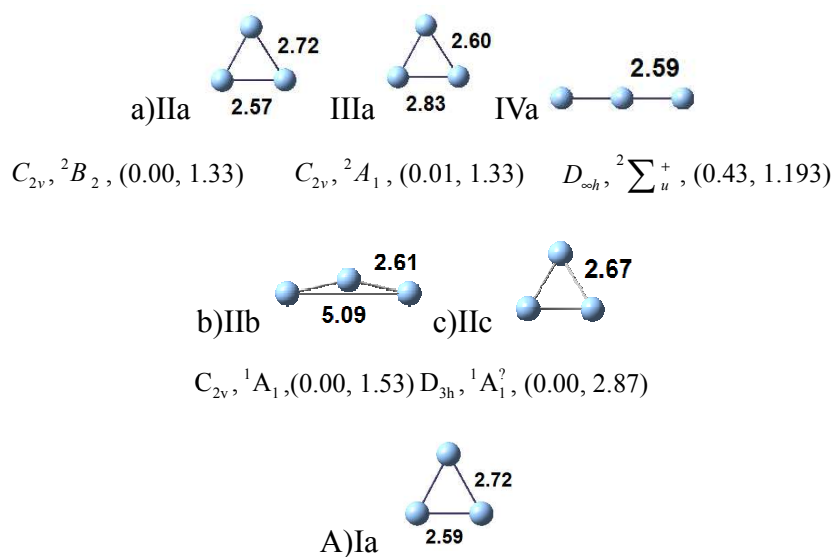


Fig. 18. The structure of trimer clusters with PBE/3-21G**: a) neutral; b) anions; c) cations. Between parenthesis are reported the relative energy, ΔE , (eV), and binding energy for atom (eV). A) neutral in water

The structure of obtuse triangle optimized with HF/LANL1MB are the angle 148.74° and the distances 3.21 and 6.18 Å, see Fig. 10 (IIa).

Used the HF/LANL2DZ for the 3 atoms clusters exist also the contraction of the bonding for the relativistic effect, see Fig. 12 (IIa).

Analyze the Fig. 17 (IIa) y 18 (IIa) I observed who the electronic correlation effects are competitively with the relativistic effects for trimer structure has been the difference for the binding of 0.04 and 2.03 Å. Moreover, compared with B3LYP/LANL2DZ where are obtained 2.69 SDD and PBE to influence of geometrical property of Ag_3 .

Except when are employed PBE/3-21G** the anion cluster are for all levels of theory the linear geometry.

For the anion cluster with DFT/PBE/3-21G** has been obtained the triangular structure less stable by 1.3 eV who linear structure [51].

To compare the DFT/B3LYP and HF, and employed LANL2DZ, have been obtained the difference of 0.21 Å, see Fig. 15 (IIIa) y Fig. 12 (IIIa).

In the case of Ag_3 the electronic correlation effects alone or complementary with relativistic effects (PBE/SDD) are strived. For anions structures the more stable are the lineal

structure, for neutral structure the obtuse-angled triangle and for the cation the equilateral triangle.

3.3. Tetramer and Pentamer Neutral, Anions and Cations

The Ag_4 structure are HOMO doubly occupied in the singlet. Compared the rhombic structure of neutral cluster in la Fig. 21 (IIIa) and the cation cluster, see Fig. 21 (IVc), optimized with HF/LANL2DZ, I observe who the distance are minor for neutral cluster who cation cluster (2.77 y 2.83 Å).

Between two central atoms, possibly on account of in part of the p atomic orbitals to bind weakly in HOMO with another atoms allowances above the greater diagonal. For such motive in the neutral cluster doubly occupied in HOMO the distance between two atoms are less who in the cation.

The same to present for the silver when are performed with PBE/SDD, see Fig. 26 (IIIa y IIIc) and the optimized cluster with MP2, see Fig. 25 (IIIa y IIIc).

For the rhomboidal structure, the experimental distance are reported in [39] is 2.79 Å comparison with 2.81 Å obtained in the present work, see Fig. 24 (IIIa). The form T is very stable, successively for rhomboidal and lineal structure.

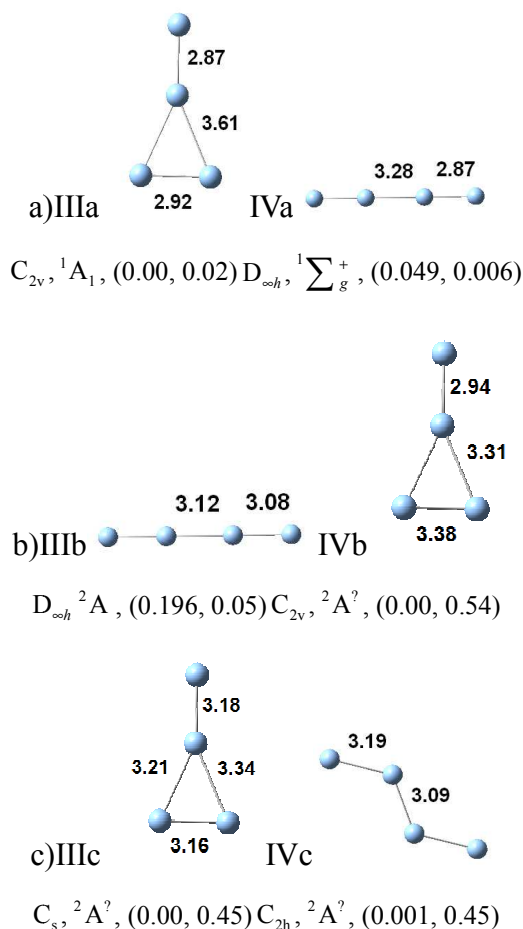


Fig. 19. The structure of Ag_3 clusters with HF/LANL1MB: a) neutral; b) anions; c) cations. Between parenthesis are reported the relative energy, ΔE , (eV), and binding energy for atom (eV)

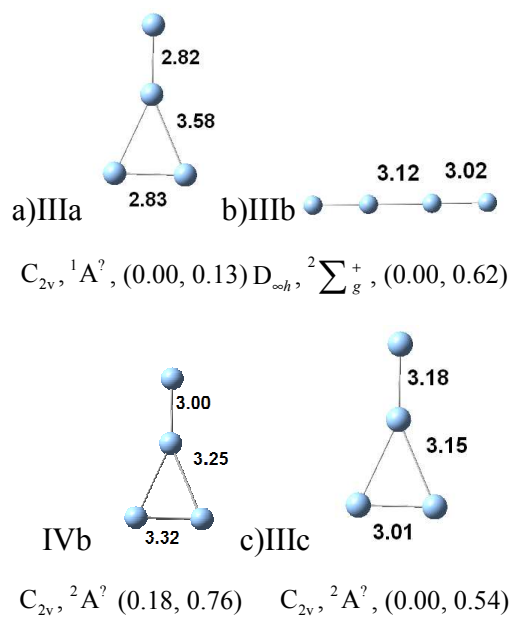


Fig. 20. The structure of Ag_4 clusters with HF/LANL2MB: a) neutral; b) anions; c) cations. Between parenthesis are reported the relative energy, ΔE , (eV), and binding energy for atom (eV)

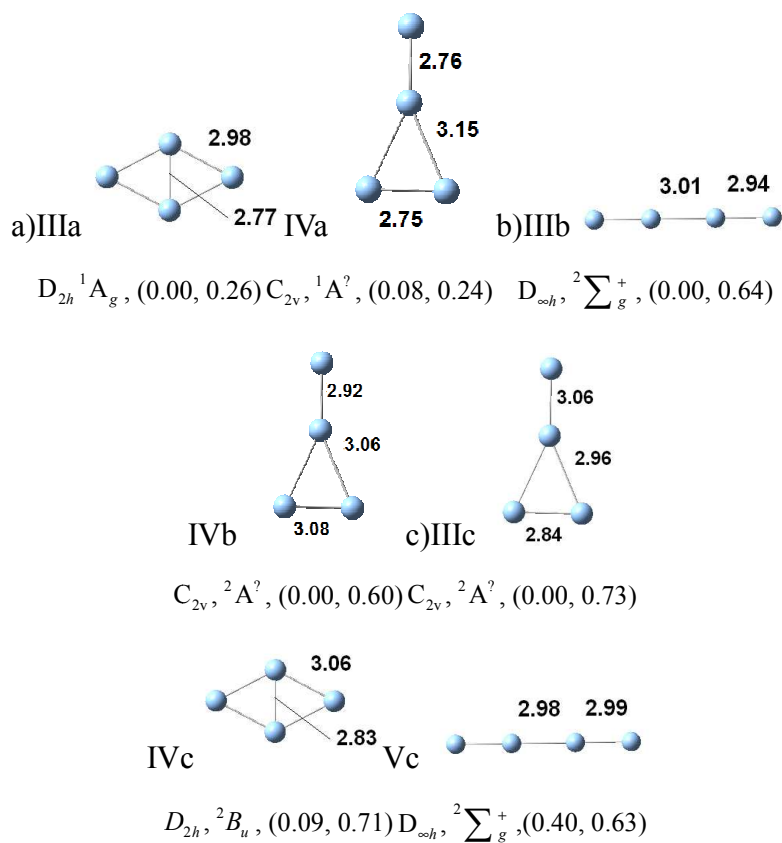


Fig. 21. The structure of Ag_4 clusters with HF/LANL2DZ: a) neutral; b) anions; c) cations. Between parenthesis are reported the relative energy, ΔE , (eV), and binding energy for atom (eV)

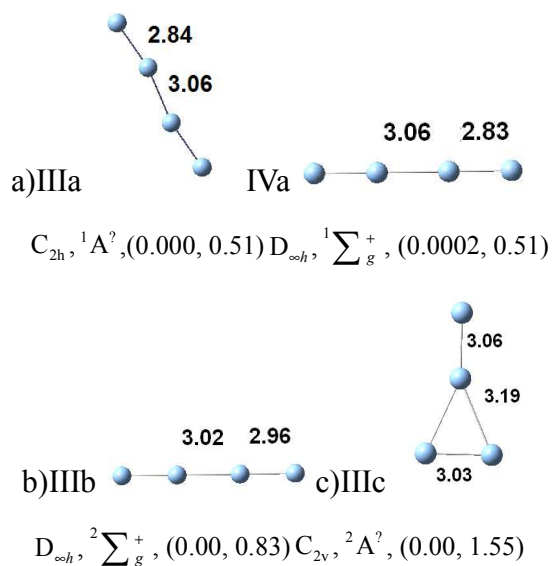


Fig. 22. The structure of Ag_4 clusters with B3LYP/LANL1MB: a) neutral; b) anions; c) cations. Between parenthesis are reported the relative energy, ΔE , (eV), and binding energy for atom (eV)

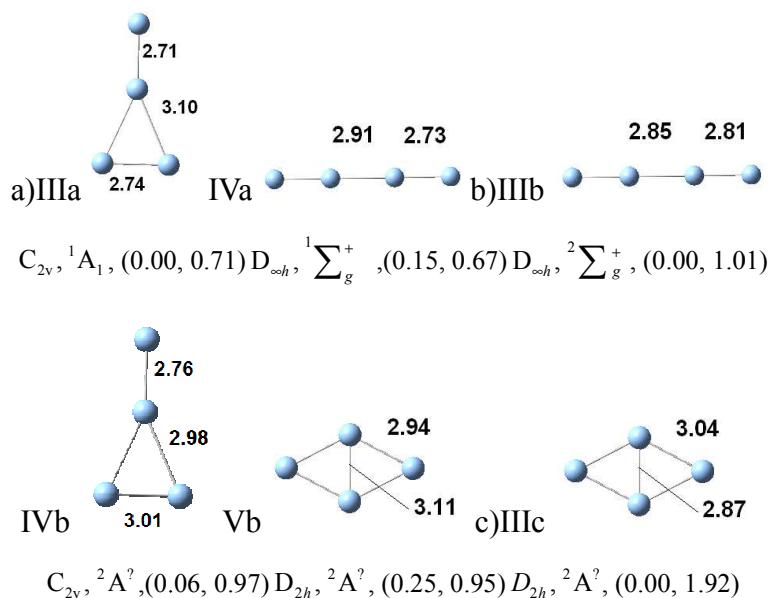
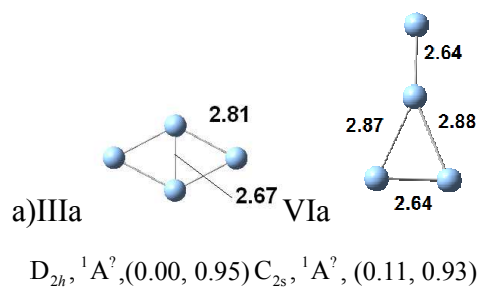


Fig. 23. The structure of Ag_4 clusters with B3LYP/LANL2MB: a) neutral; b) anions; c) cations. Between parenthesis are reported the relative energy, ΔE , (eV), and binding energy for atom (eV)



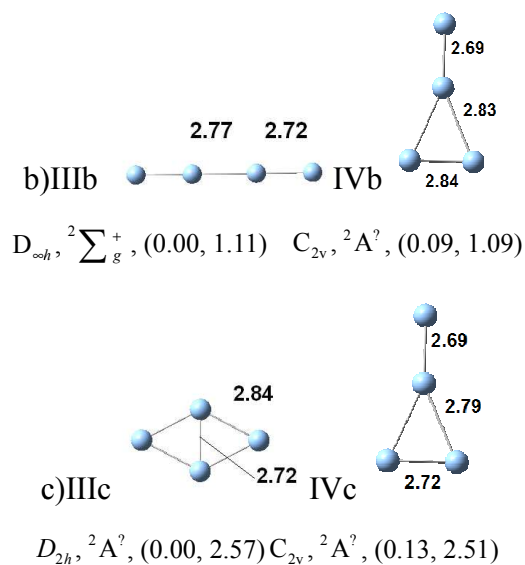


Fig. 24. The structure of Ag_4 clusters with B3LYP/LANL2DZ: a) neutral; b) anions; c) cations. Between parenthesis are reported the relative energy, ΔE , (eV), and binding energy for atom (eV)

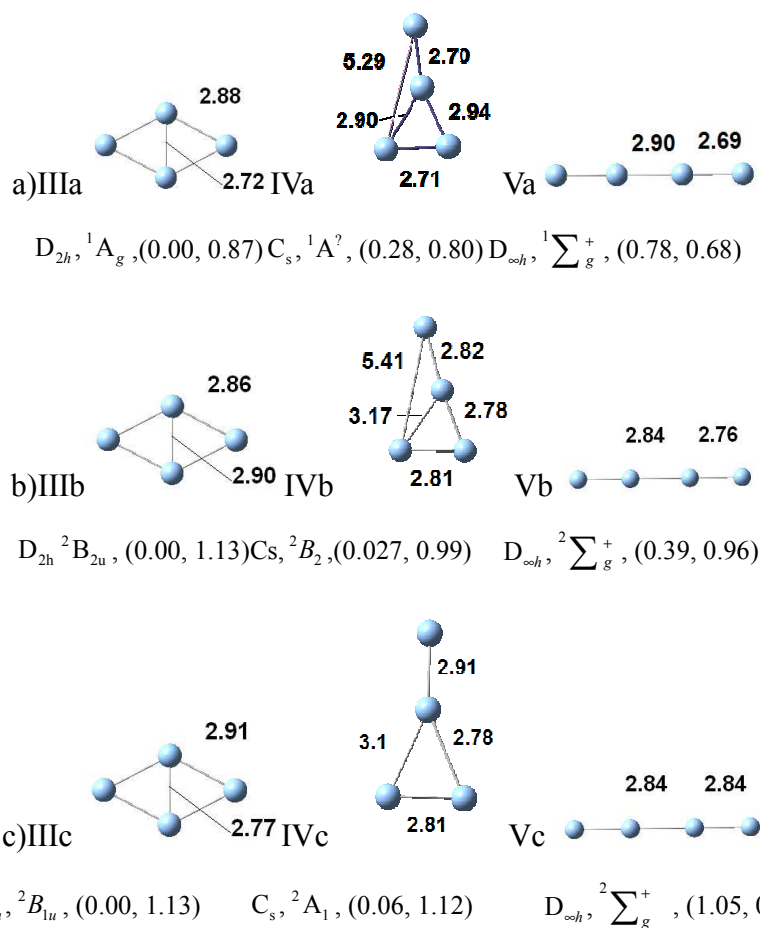


Fig. 25. The structure of Ag_4 clusters with MP2/LANL2DZ: a) neutral; b) anions; c) cations. Between parenthesis are reported the relative energy, ΔE , (eV), and binding energy for atom (eV)

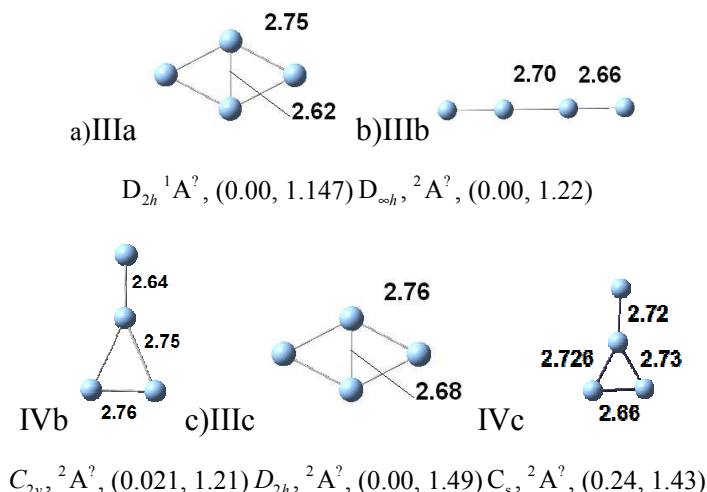


Fig. 26. The structure of Ag_4 clusters with PBE/SDD: a) neutral; b) anions; c) cations. Between parenthesis are reported the relative energy, ΔE , (eV), and binding energy for atom (eV)

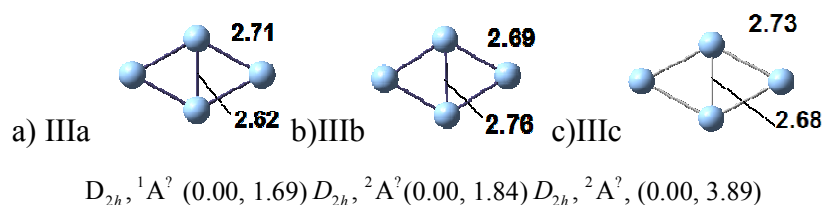


Fig. 27. The structure of Ag_4 clusters with PBE/3-21G**: a) neutral; b) anions; c) cations. Between parenthesis are reported the relative energy, ΔE , (eV), and binding energy for atom (eV)

In [44] has been reported the distance for Ag_4^- anions cluster obtained with SCF 1e—RECP-CVC. Romboidal the 2.789 Å and 2.838 Å with difference of 0.02 Å of the distance obtained optimized with PBE/SDD, but less who 2.69 Å obtained with DFT and PBE AND 3-21G**.

For Ag_4 neutral cluster are performed with HF/LANL2DZ and B3LYP/LANL2DZ

Comparison the distance between atoms in the neutral cluster with rombic structure optimized rebound who contraction for electronic correlation is 0.17 Å and 0.10 Å,

see Fig. 21 y 24 (IIIa y IIIa).

For cations cluster in Fig. 21 and 24 (IIIb, IVb, IIIb y IIIc) the the contraction are 0.25 Å, greater who in the neutral clusters. For cation in water the distance are less than in gas phase, but neutral cluster are more distance than in gas phase.

Between the neutral structure optimized with 5 atoms with DFT/B3LYP/LANL2DZ, the trapezium is better stable than pyramidal with square base so how are moderate in [18] how experimental date.

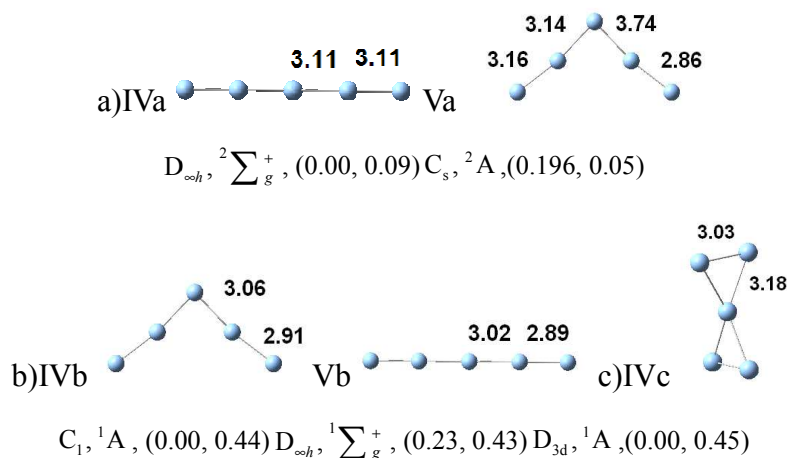


Fig. 28. The structure of Ag_5 clusters with HF/LANL1MB: a) neutral; b) anions; c) cations. Between parenthesis are reported the relative energy, ΔE , (eV), and binding energy for atom (eV)

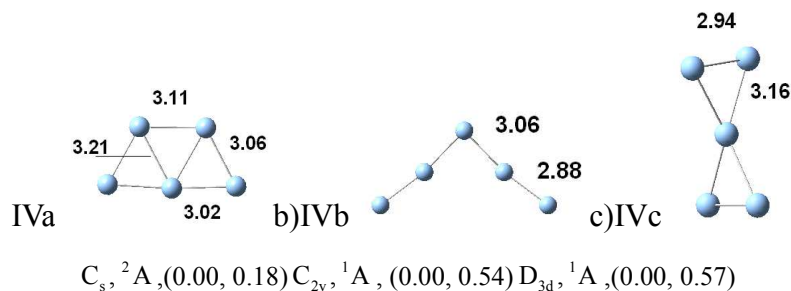


Fig. 29. The structure of Ag_5 clusters with HF/LANL2MB: a) neutral; b) anions; c) cations. Between parenthesis are reported the relative energy, ΔE , (eV), and binding energy for atom (eV)

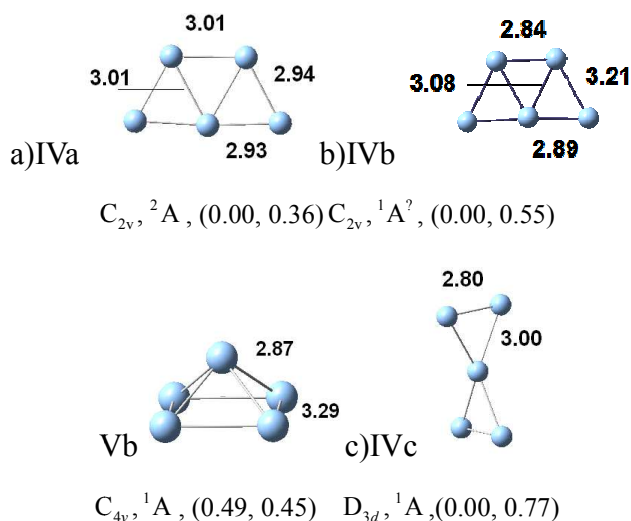


Fig. 30. The structure of Ag_5 clusters with HF/LANL2DZ: a) neutral; b) anions; c) cations. Between parenthesis are reported the relative energy, ΔE , (eV), and binding energy for atom (eV)

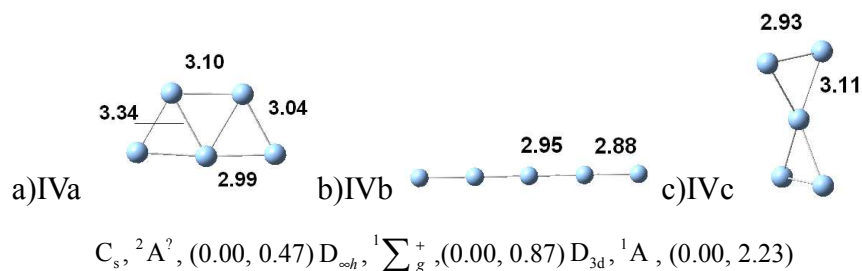


Fig. 31. The structure of Ag_5 clusters with B3LYP/LANL1MB: a) neutral; b) anions; c) cations. Between parenthesis are reported the relative energy, ΔE , (eV), and binding energy for atom (eV)

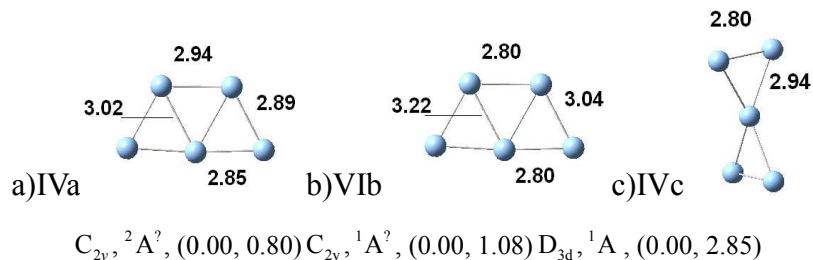


Fig. 32. The structure of Ag_5 clusters with B3LYP/LANL2MB: a) neutral; b) anions; c) cations. Between parenthesis are reported the relative energy, ΔE , (eV), and binding energy for atom (eV)

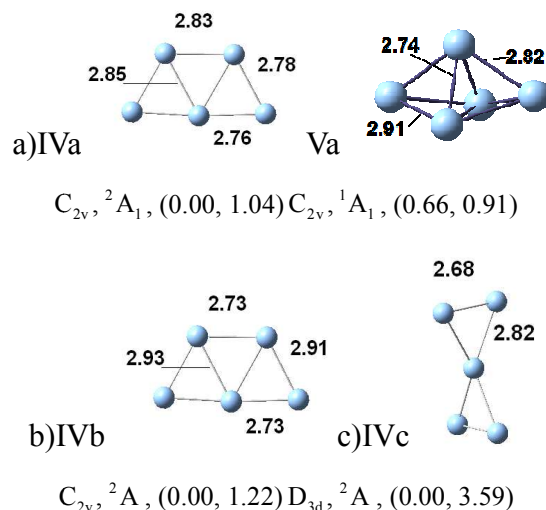


Fig. 33. The structure of Ag_5 clusters with B3LYP/LANL2DZ: a) neutral; b) anions; c) cations. Between parenthesis are reported the relative energy, ΔE , (eV), and binding energy for atom (eV)

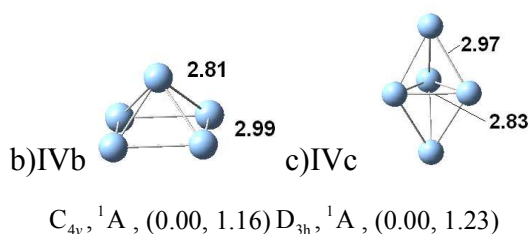


Fig. 34. The structure of Ag_5 clusters with MP2/LANL2DZ: a) neutral; b) anions; c) cations. Between parenthesis are reported the relative energy, ΔE , (eV), and binding energy for atom (eV)

I observe the influence of the relativistic effects for Ag_5^+ employed HF/LANL1MB, HF/LANL2MB and HF/LANL2DZ with the contraction of 0.09 and 0.06 Å in distance, see Fig. 28 (IVc), 29 (IVc) and 30 (IVc). With B3LYP the difference between distance in $C_{2v}, {}^1A_1$ is the 0.16 Å with Ag_5 optimized with HF/LANL2DZ, see Fig. 21 (Va) and Fig. 33 (IVa).

On change comparatively the variation of distance between the structure optimized trapezoidal with B3LYP/LANL1MB and B3LYP/LANL2DZ the difference are 0.26 Å who to oppose who relativist effect are greater who the electronic correlation, the plan structure has been more stable when the bipiramydal structure with triangle base, so report in experimental data [18].

This debit of hybridization between $4d$ y $5s$ that to favor the planar structure. The hibridization are interesinteresting for the relativistic effects in Au, Cu and silver, in this case particular [59].

Fort he silver plata Ag_7 rebound to be who the planar structure is stable with diminution in distance, so how Au_7 [67].

4. Biding Energy for Atom

Is important to study the biding energy for atom because to refer at stability of clusters. Are graphical the value of the

biding energy of the neutral cluster, anions and cations Fig. 35-43 calculated with $\frac{E_b}{n} = (nE_1 - E_n)/n$ where E_1 and E_n are the total energy for the neutral species optimized for un atom and n atoms;

$$\frac{E^\pm}{n} = [(n-1)E_1 + E_1^\pm - E_n^\pm]/n$$

where E_1^\pm and E_n^\pm are the total energy for the positive and negative for un atom and n atoms.

In Fig. 35 are presented the results obtained for the neutral clusters of Ag_n ($n=1-5$). Tendency in the values of biding energy of the cluster augment with the number of atoms employed the HF/LANL2DZ level. Th estructure T for Ag_4 optimized with LANL2MB and LANL1MB is less stable who the triangular, rombic and lineal structure

In Jahn-Teller for the neutral clusters Ag_3 optimized with HF/LANLEDZ resulte who el isomer more stable are the optuse triangle with the biding energy with 0.193 eV, successive for the lineal structure with biding energy of 0.191 eV and, for the last is the $C_{2v}, {}^2A_1$ structure with 0.161 eV, see Fig. 32 (IIa, IIIa y IVa), when this are not the experimental reported where the 2B_2 is better stable who 2A_1 [48, 50].

In the Fig. 19 has been optimized the $D_{\infty h}, \sum_g^+$ lineal with HF/LANL1MB, for Ag_4 and are the value 0.013 V who

the T form with $C_{2v}, ^1A_1$ symmetry Fig. 19 (IIIa).

For Ag_4 optimized with HF/LANL2DZ the structure more stable is rhombic with the little difference 0.12 eV, for binding energy, with the T form with $C_{2v}, ^1A_1$ symmetry, see Fig. 21

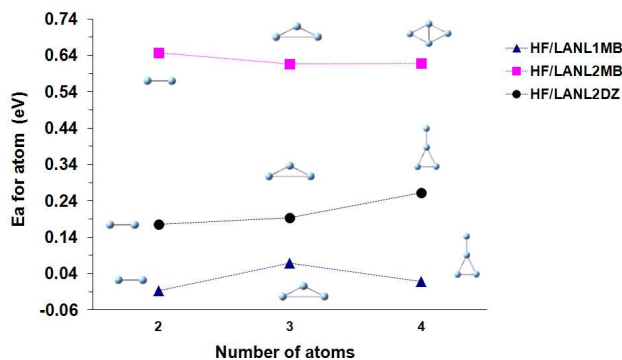


Fig. 35. Binding energy for atom for neutral clusters employed HF. Vs. Number of atom for clusters. The most stable structure. [80]

For anions clusters, see Fig.36, for Ag_3 and Ag_4 , the form more stable are lineal. For Ag_4 anion optimized with LANL1MB the lineal form is more stable who T form with 0.08 eV only see Fig. 19.

The distribution of charge after to remove 1 electron for Ag_4^+ to favor the T form how more stable with binding energy 0.73 eV, the act of following for rhombic and lineal structure with 0.71 and 0.63 eV.

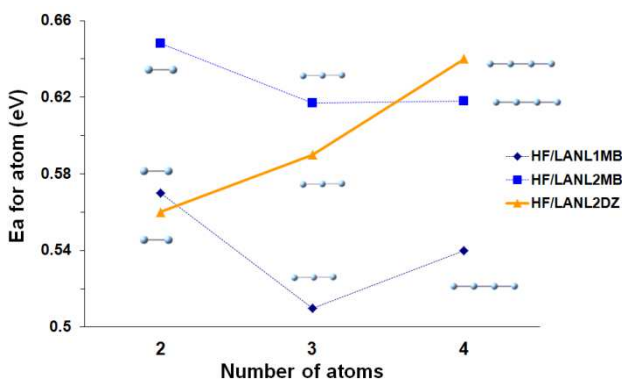


Fig. 36. Binding energy for atom for neutral clusters employed HF. Vs. Number of atom for clusters. The most stable structure. [80]

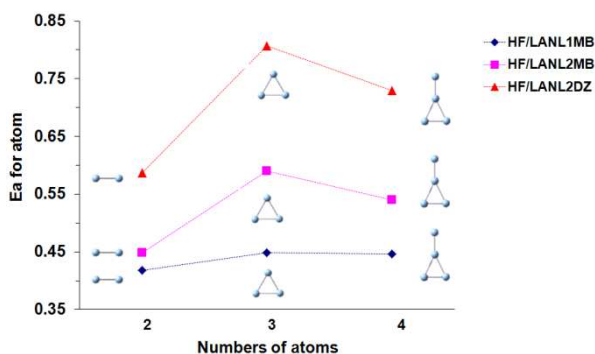


Fig. 37. Binding energy for atom for neutral clusters employed HF. Vs. Number of atom for clusters. The most stable structure. [80]

In the Fig. 38 are graphicate the value of binding energy for the neutral of silver with 2 and 4 atoms. When are optimized the cluster with B3LYP/LANL1MB has been obtained less value for Ag_n ($n = 2-4$) 0.446 eV, 0.403 eV and 0.511 eV, see Fig. 38.

The value of binding energy for dimer clusters obtained with PBE/SDD and B3LYP/LANL2DZ of 0.876 eV and 0.776 eV near of the data experimental [60].

The binding energy obtained for the isomer $^2B_2, ^2\Sigma_u^+$ and 2A_1 obtained Ag_3 with B3LYP/LANL2DZ has been 0.740 eV, 0.705 y 0.738 eV.

In this case has been different to the experimental results where the difference between 2B_2 and 2A_1 are the 0.022 eV [61] and, between 2B_2 y $^2\Sigma_u^+$ are 0.15 eV in [38] or the value 0.85 eV reported in [48].

When has been optimized with MP2/LANL2DZ the difference between 2A_1 and 2B_2 is the 0.001 eV only the binding energy are the same 0.6 eV. For PBE/3-21G** has been see greater values, see Fig. 38, and the binding energy concured with the report in the literatura [60].

For Ag_4^- optimized with B3LYP/LANL2MB the $D_{\infty h}, ^2\Sigma_g^+$ are binding energy for atom of 1.01 eV compared with de T form who are 0.97 eV and $D_{2h}, ^2B_{2u}$ with 0.95 eV (see Fig. 23).

Employed PBE/SDD level of theory for obtained Ag_4^- the difference between lineal structure end T form are 0.01eV, implicated who energy for separation the two structure is almost equal. On the contrary, employed MP2/LANL2DZ level of theorie in the Fig. 25 see who lineal structure Ag_4^- are the binding energy minor (0.96 eV) who structure $D_{2h}, ^2B_2$ with 0.99 Ev and rhombic structure $D_{2h}, ^2B_{2u}$ with 1.13 eV.

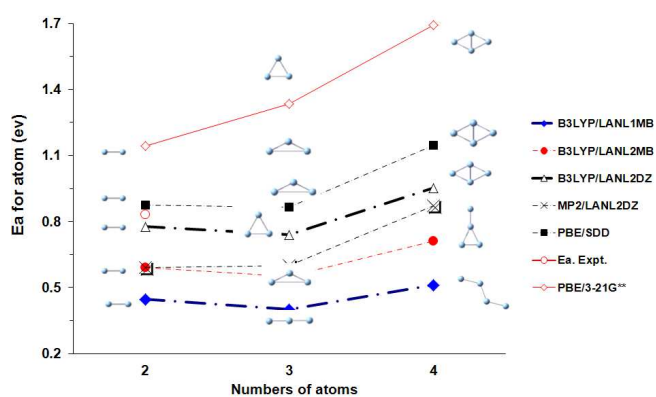


Fig. 38. Binding energy for atom for neutral clusters employed DFT. Vs. Number of atom for clusters. E_a ,experimental [36].The most stable structure.[80]

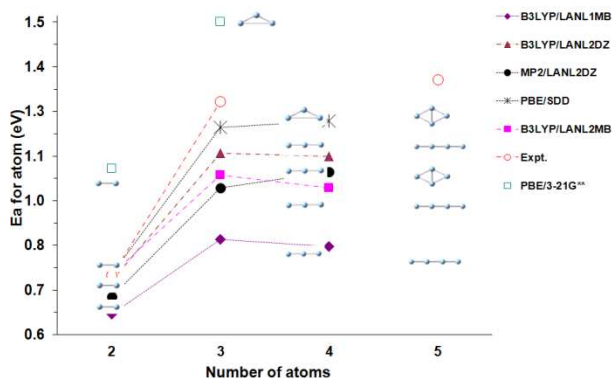


Fig. 39. Binding energy for atom for neutral clusters employed DFT. Vs. Number of atom for clusters. $E_{a, \text{experimental}}$ [36]. The most stable structure. [80]

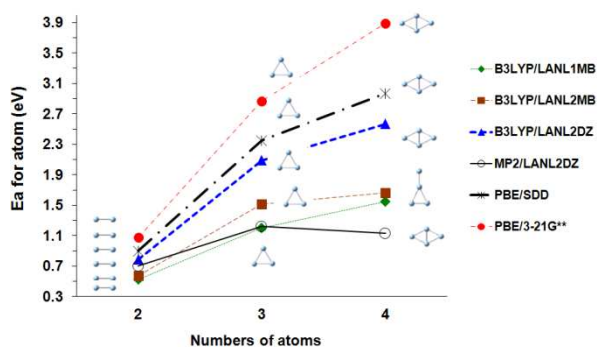


Fig. 40. Binding energy for atom for neutral clusters employed DFT. Vs. Number of atom for clusters. The most stable structure. [80]

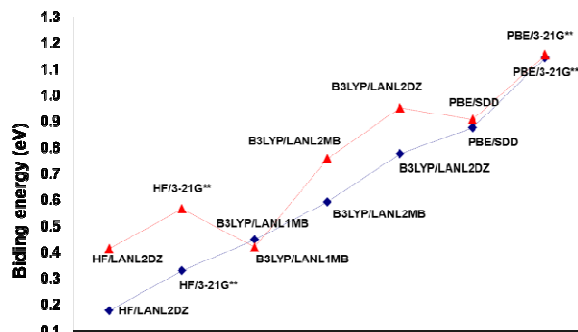


Fig. 41. Binding energy for atom for neutral dimer clusters in water in red in water and blue in gas phase. Vs. Number of atom for clusters. The most stable structure.

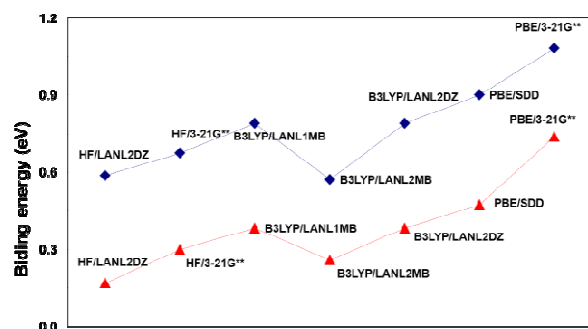


Fig. 42. Binding energy for atom for dimer cations clusters in water in red in water and blue in gas phase. Vs. Number of atom for clusters. The most stable structure.

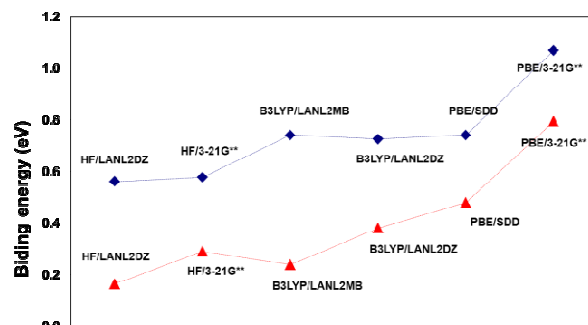


Fig. 43. Binding energy for atom for dimer anions clusters in water in red in water and blue in gas phase. Vs. Number of atom for clusters. The most stable structure.

5. Ionization Potential and Electronic Affinity

5.1. Adiabatic Electronic Affinity and Vertical

In this section are show the values obtained for electronic affinity and ionization potential for compared with the theoretic result and experimental data and see which of the effects relativistic or electronic correlation interfere in this proprieties.

The calculus for the electronic affinities has been calculated with $A = E_n - E_n^-$, where E_n is the total energy for the neutral species optimized and E_n^- is the total energy for the anion species after optimized.

How to observe in the Fig. 44 and 45 the values for electronic affinity are distant for the experimental data and are not the same tendency for the clusters optimized with HF and LANL1MB, LANL2MB and LANL2DZ bases.

This a shop sign who HF are not describet fitly the adiabatic electronic affinity for the silver clusters already who solely consider the relativistic effects and giving who understimade the difference of energy of the Ag_n and Ag_n^- .

The difference for the silver clusters Ag_3 are 1.5 eV for Ag_2 are 0.43 eV and Ag_4 0.32 eV, see Fig. 46.

Compared Fig. 44 and 45 has been observed who the results obtained for vertical electronic affinity concurred with the adiabatic electronic affinity motive for which is advisable employed vertical electronic affinity.

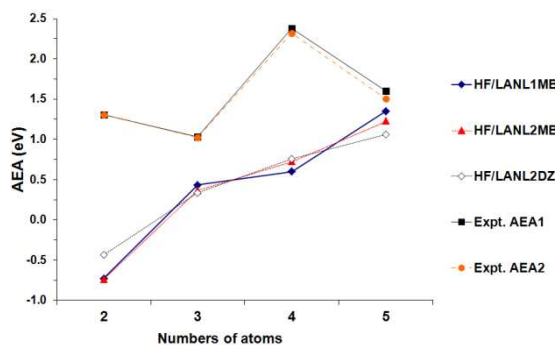


Fig. 44. Adiabatic electronic affinity for silver cluster employed. Vs. Number of atoms in the cluster. AEA1 experimental [61-63]. AEA2 experimental [37]. [80]

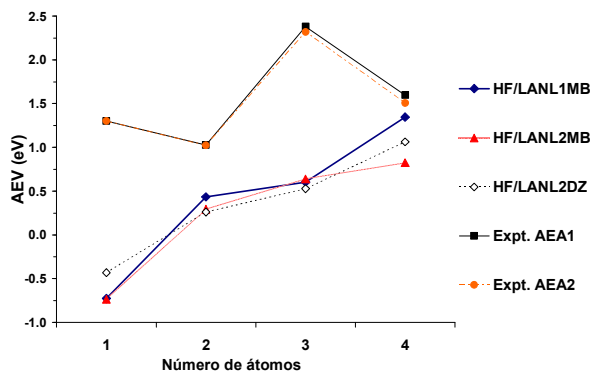


Fig. 45. Adiabatic electronic affinity for silver cluster employed HF. Vs. Number of atoms in the cluster. AEA1 experimental [61- 63]. AEA2 experimental [37], [80]

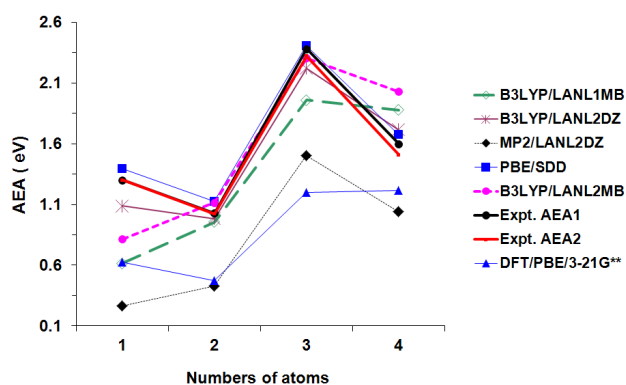


Fig. 46. Adiabatic electronic affinity for silver cluster employed DFT. Vs. Number of atoms in the cluster. AEA1 experimental [61, 63]. AEA2 experimental [37], [80]

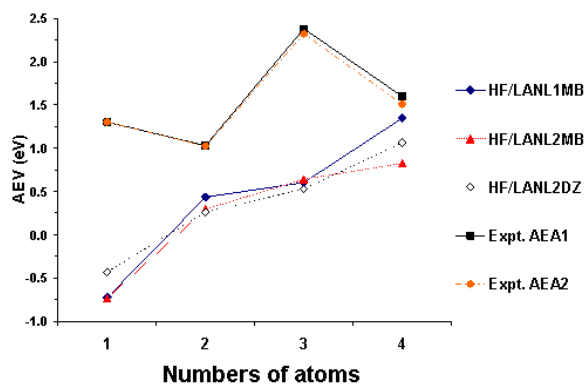


Fig. 47. Adiabatic electronic affinity for silver cluster employed DFT. Vs. Number of atoms in the cluster. AEA1 experimental [61, 63]. AEA2 experimental [37], [80]

Introduced the electronic correlation effects with PBE functional and the relativistic effects SDD has been obtained, for the adiabatic electronic affinity, value very nears of the experimental data reported in [62-64, 48] for Ag_n ($n=1-4$) (see Fig. 44 and 45). With the electronic correlation effects PBE/3-21G**, the values are very distant of the experimental data, see Fig. 46 and 47.

With B3LYP functional and LANL2DZ has been obtained good results for the adiabatic electronic affinity, Fig. 46 and

47.

The results obtained in this work for the silver cluster optimized with MP2/LANL2DZ concurred with the results in the literature employed MP2 and LANL2DZ [65].

If compared the results obtained with DFT/PBE/SDD, DFT/PBE/3-21G** and HF/LANL2DZ the relativistic effects only, are not much influenced in adiabatic electronic affinity and neither the electronic correlation effects with PBE functional.

Analyzed the data obtained with DFT/B3LYP/LANL2DZ and DFT/PBE/SDD I see little variation.

5.2. Vertical and Adiabatic Ionization Potential

The adiabatic ionization potential are defined how the energy of transition in origin between the basal state of cation and the basal state of neutral with $I = E_n^+ - E_n^-$, where E_n^+ is the total energy of species of cations after optimization the structure and E_n^- is the total species neutral optimized [25].

Tendency of the clusters obtained with HF, see Fig. 45 and 46 is do not equal with the experimental data [66,18]. The values of ionization potential are extensive comparable with electronic affinity [27, 67].

With LANL1MB and LANL2MB change of the data for dimer and trimer clusters are the same.

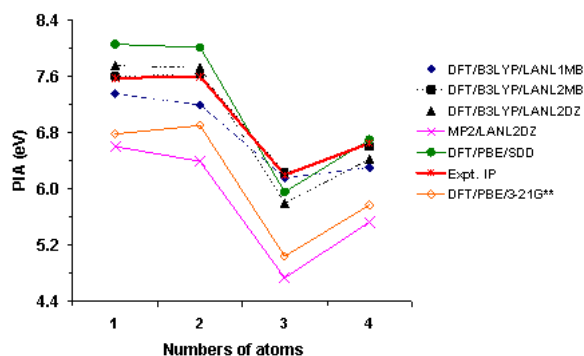


Fig. 48. Adiabatic electronic potential for silver cluster employed DFT. Vs. Number of atoms in the cluster. Experimental potential of ionization [6, 46], [80]

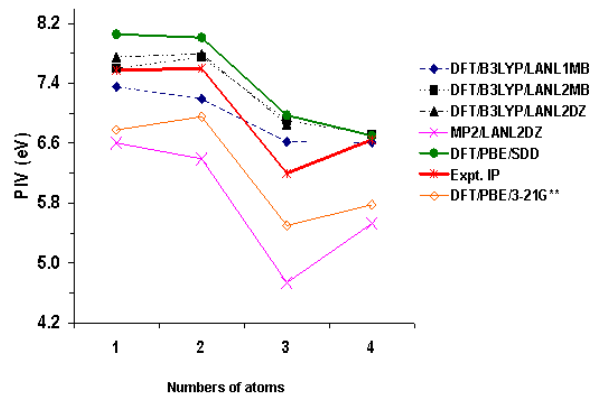


Fig. 49. Adiabatic electronic potential for silver cluster employed DFT. Vs. Number of atoms in the cluster. Experimental potential of ionization [6, 46], [80]

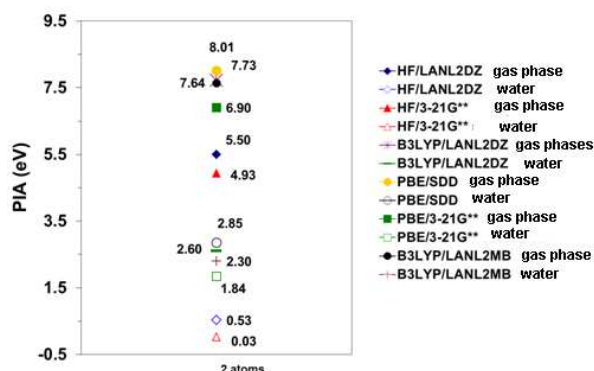


Fig. 50. Adiabatic electronic potential for silver dimer cluster in water and gas phase. The graphics is change

With see the Fig 48 has been obtained good results when are employed B3LYP/LANL2MB. The diference with experimental data are de 0.03 eV for one atom, two atoms and three atoms and, 0.14 eV for fourth atoms clusters.

When are employed B3LYP/LANL2DZ level of theorie are obtained 7.75 eV estimated with 7.57 eV, the experimental data for one atom, 7.72 eV compared with 7.6 eV, the experimental data for two atoms, see Fig.49.

The better result are obtained with B3LYP and are near of the jellium model (SJBM). Are better PBE/SDD who PBE/3-21G**.

The electron are ionized of the feeble biding orbital, see Fig 48 and 49. The IP for three atoms are less who for over.

6. Frecuencias

How see in Table 1 the values better near of the experimental data for two atoms anion and cation has been

obtained employed PBE/SDD. For neutral dimer employed PBE/3-21G** are obtained 199.08 cm^{-1} forehead to 192.4 (5), the experimental data (see Table 1) continued for the DFT/PBE/SDD level.

Tabla 1. The armonic frecuencia (in cm^{-1}) of the mas stable silver clusters.

Ag_4	Ag_4^-	Ag_4^+	Ag_3	Ag_3^-	Ag_3^+
			161.1 (157.9) ^a		
34.16 ^b	71.57 ^b	15.56 ^b	13.25 ^b	28.44 ^b	110.80 ^b
71.58 ^b	134.57 ^b	71.32 ^b	112.71 ^b	89.96 ^b	110.89 ^b
76.25 ^b	166.53 ^b	84.80 ^b	159.16 ^b	156.12 ^b	167.53 ^b
100.30 ^b		87.45 ^b			
152.35 ^b		127.64 ^b			
174.99 ^b		160.11 ^b			
38.44 ^c	15.23 ^c	18.44 ^c	11.79 ^c	34.94 ^c	117.87 ^c
82.89 ^c	22.95 ^c	82.03 ^c	126.41 ^c	107.76 ^c	118.49 ^c
186.73 ^c	28.65 ^c	94.76 ^c	171.33 ^c	178.23 ^c	174.66 ^c
92.77 ^c	78.31 ^c	103.86 ^c			
164.57 ^c	144.02 ^c	146.94 ^c			
186.73 ^c	178.47 ^c	169.87 ^c			
		14.87 ^d	87.72 ^d	42.97 ^d	118.71 ^d
		91.02 ^d	114.58 ^d	128.23 ^d	118.71 ^d
		97.31 ^d	197.20 ^d	196.12 ^d	184.06 ^d
		115.05 ^d	5.63 ^e		
		158.53 ^d	80.55 ^e		
		178.05 ^d	91.70 ^e		

^aexperimental data [29]^bthe date of the present work with DFT/B3LYP/LANL2DZ level of theorie

^cthe date of present work with DFT/PBE/SDD ^dthe date of the present work with DFT/PBE/3-21G** level of theorie

^ethe date of presen work with HF/LANL2DZ

Tabla 2. Energy, adiabatic electronic potential, adiabatic electronic afinityof the clusterin solvent ($\epsilon = 78.39$). Are employed PCM.

No. atoms	Method	E_T	E_{cat}	E_{anion}	I_{adiab}	AE_{adiab}
	PCM ($\epsilon = 78.39$)					
1	DFT/PBE/3-21G**	140839.45	-140837.14	-140841.38	2.31	1.93
2		-281681.21	-281678.06	-281682.42	3.14	1.21
1	DFT/PBE//SDD	-3998.80	-3995.52	-4001.71	3.28	3.75
2		-7999.42	-7995.27	-8001.47	4.52	
1	DFT/B3LYP/ LANL2DZ	-3966.45	-3963.38	-3969.20	1.77	2.75
2		-7934.50	-7930.60	-7936.41	2.60	1.91
1	DFT/B3LYP/ LANL2MB	-3966.31	-3963.37	-3968.84	2.94	2.53
2		-7933.79	-7930.19	-7935.62	3.60	1.83
1	HF/3-21G**	-140786.77	-140785.52	-140787.28	1.25	0.51
2		-281574.21	-281572.89	-281574.63	1.33	0.41
1	HF/LANL2DZ	-3942.88	-39.41.179	-3943.91	1.70	1.04
2		-7886.22	-7884.39	-7887.12	1.83	0.89

E_T – total energy of Ag_1 y Ag_2

E_{cat} energy of Ag_1 y Ag_2 cation

E_{anion} – eneryof Ag_1 y Ag_2 anion

I_{adiab} –adiabatic potential for Ag_1 and Ag_2

AE_{adiab} –adiabatic afinity for Ag_1 and Ag_2

In the Table 3 are see the anion dimer obtained with PBE/SDD and HF/LANL2DZ

Tabla 3. The armonic frecuencia (in cm^{-1}) of the mas stable silver clusters in gas phase, [80]

Métodos	Ag ₂	Ag ₂ ⁻	Ag ₂ ⁺
Experimental[20, 21]	192.4(5) ^{a,b}	145.0 ^c	135.8 ^c
DFT/PBE/3-21G**	199.07	165.96	141.13
DFT/PBE/SDD	185.94	134.22	131.58
DFT/B3LYP/LANL2DZ	177.06	125.61	124.16
DFT/B3LYP/LANL2MB	146.45	125.61	124.16
HF/3-21G**	141.12	97.26	94.48
HF/LANL2DZ	149.32	88.59	91.30

^a experimental [28]

^b experimental [29]

^c experimental [30]

Tabla 4. The frecuencias obtained for the silver cluster in acuos solution with the PCM ($\epsilon = 78.39$) model.

MÉTODOS solvatación ($\epsilon = 78.39$)	Ag ₂	Ag ₂ ⁻	Ag ₂ ⁺
DFT/PBE/3-21G**	188.15	120.1191	157.79
DFT/PBE/SDD	175.53	-53.28	138.12
DFT/B3LYP/LANL2DZ	162.00	94.47	133.35
DFT/B3LYP/LANL2MB	146.45	94.47	133.35
HF/3-21G**	111.75	46.23	95.51
HF/LANL2DZ	115.76	-17.85	85.39

Tabla 5. The values of HOMO, LUMO, and gap for the Ag₂ clusters in the gas phase.[80]

Method	HOMO (eV)	LUMO (eV)	HOMO-LUMO gap (eV)
DFT/PBE/3-21G**	-4.290	-2.379	1.911
DFT/PBE//SDD	-5.262	-3.235	2.027
DFT/B3LYP/LANL2DZ	-5.558	-2.653	2.905
DFT/B3LYP/LANL2MB	-5.559	-2.845	2.714
HF/3-21G**	-5.392	0.253	5.139
HF/LANL2DZ	-5.949	0.030	5.979

Tabla 6. Values of HOMO, LUMO, and gap for the Ag₂ clusters obtained in acuos solution employed PCM model with $\epsilon = 78.39$.

SOLVATATION ($\epsilon = 78.39$)			
Method	HOMO (eV)	LUMO (eV)	HOMO-LUMO gap (eV)
DFT/PBE/3-21G**	-3.230	-1.021	2.209
DFT/PBE//SDD	-4.230	-1.836	2.394
DFT/B3LYP/LANL2DZ	-4.572	-1.276	3.295
DFT/B3LYP/LANL2MB	-4.170	-1.259	2.912
HF/3-21G**	-4.300	1.682	2.618
HF/LANL2DZ	-5.175	1.217	3.958

Tabla 7. Values of HOMO, LUMO, and gap for the Ag₃ clusters obtained in the gas phase.[80]

Method	HOMO (eV)	LUMO (eV)	HOMO-LUMO gap (eV)
DFT/PBE/3-21G**	-4.129	-2.814	1.314
DFT/PBE//SDD	-5.136	-3.600	1.536
DFT/B3LYP/LANL2DZ	-5.419	-3.039	2.380
DFT/B3LYP/LANL2MB	-5.411	-3.164	2.247
HF/3-21G**	-5.045	-3.164	1.881
HF/LANL2DZ	-5.354	-3.164	2.190

Tabla 8. Values of HOMO, LUMO, and gap for the Ag₃ clusters obtained in the solvent.

SOLVATACIÓN ($\epsilon = 78.39$)			
Métodos	HOMO (eV)	LUMO (eV)	HOMO-LUMO gap (eV)
DFT/PBE/3-21G**	-2.284	-1.268	1.576
DFT/PBE//SDD	-5.136	-3.600	1.536
DFT/B3LYP/LANL2DZ	-4.045	-1.463	2.582
DFT/B3LYP/LANL2MB	-5.411	-3.164	2.247
DFT/B3LYP/LANL1MB	-3.268	-1.178	2.090
HF/3-21G**	-5.354	0.028	5.382

7. Hardness

Are calculated hardness with the objective see the reactivity of the cluster taken in account the relativistic effects and electronic correlation and see what silver cluster digest how soft acid r soft base u hard acid or hard base. The value of hardnees ar in Fig. 51 and52. And are employed $\eta = (I-A)/2$.

With the HF I observ who the more reactive are the structure with for atoms.

When I empolyed LANL1MB the 1.64 eV are obtained, for the LANL2DZ level the value are 1.70 eV, see Fig.51.

To be observed who the reactivity increment with el number of atoms in the cluster and not exist the variation pair unequal. The Ag₃ optimised with HF/LANL2DZ is near of the experimental hardness.

See de hardness experimental in Fig. 42, 50 and 47 [62, 64 68, 66, 18].

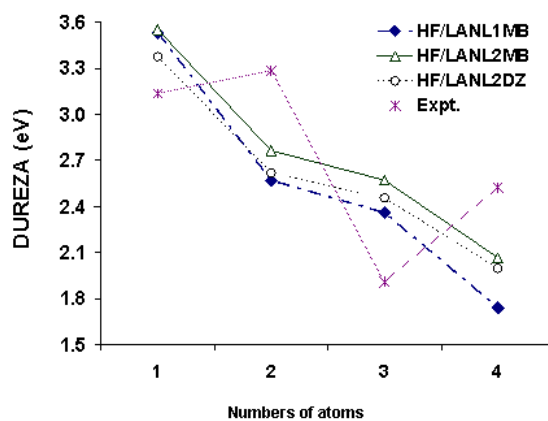


Fig. 51. Hardness (η) for the silver clusters employed HF. Vs. Number of the atoms in the cluster. , [80]

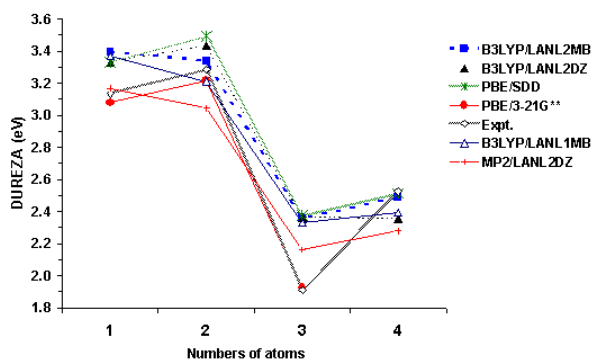


Fig. 52. Hardness (η) for the silver clusters employed DFT. Vs. Number of the atoms in the cluster. [80]

In the Fig.51 I see the best reactive are three atoms and for atoms.

In the Table 7 and 8 are the value obtained for the difference HOMO-LUMO (gap) for the clusters employed the Klopman theorie.[68].

Are calculated the HOMO-LUMO with:

$$\text{HOMO-LUMO} = (-E_{\text{HOMO}}) - (-E_{\text{LUMO}})$$

E_{HOMO} = the energie of the orbital high occupied

E_{LUMO} = the energie of the orbital low occupied.

The value obtained in the gas phase are smaller in 0.2-0.3 eV nearly with respect of the values in aqueous solution, it who oppose who the solvent make that increase the difference HOMO-LUMO.

With HF/LANL2DZ and HF/3-21G* has been obtained less values of gap with 2.521 and 2.021 eV who in gas phase.

In the water the values are different and are not experimental data.

8. Conclusions

Introducing the electronic correlation effects without relativistic effect with the PBE functional and the 3-21G** has been obtained the best results of 2.53 Å, compared with PBE/SDD with which has been obtained 2.57 Å for neutral dimer.

Of where has been concluded who the electronic correlation effects modify more in the distance between the clusters than the relativistic effects.

The anion clusters almost all case are the lineal form how the most stable, the cation of equilateral triangle and isosceles.

At make additions un electron the clusters of two and for atoms optimized with HF are better stable what of the three atoms, in barter for the cation cluster at remove un electron perform who the cluster with pair number are less stable who the cluster with unequal number.

Not be able make the same for the clusters optimized introduce the electronic correlation, in this case the charge are uniformly disposed between the three atoms in the lineal form.

Introduced the density functional are included in B3LYP the LDA functional it who make what the result obtained with DFT/B3LYP/LANL2MB it be more near of the experimental data, respecting the model of jellium layer.

In this case I observed who the relativistic effects not influence in the properties how the electronic affinity and ionization potential. Compared PBE/3-21G** and PBE/SDD the electronic correlation are complementary with the relativistic effect. The MP2 are improper with the electronic affinity and ionization potential.

The results obtained with PBE/3-21G** and PBE/SDD for the frequencies are the near of the experimental data.

The values of the hardness are near of the experimental data have been obtained for PBE/3-21G** following for PBE/SDD, when the electronic correlation are important competing with the two effects the relativistic with electronic correlation. The dipole of water are influenced the properties of cluster.

References

- [1] Huda M.N.; Ray A. K.; Phys. Rev. A, 2003, 67, 013210.
- [2] Fournier R., J. Chem. Phys., 2001, 2165.
- [3] Wnag B.; Chen X.; Wang J.; Zhao J., Surface Review and Letters, 2004, 11,15.
- [4] Monti O.L.A.; Fourkas, J.T.; Nesbitt D.J., J. Phys. Chem. B, 2004, 108, 1604.
- [5] Zhang L.; Yuu J.C., Ho Yin Yip; Li Q.; Kwong K. W.; Xu A. Wu; Wong Po K.; Langmuir, 2003, 19, 10372.
- [6] Yuranava T.; Rincon A.G.; Bozzi A.G.; Parra S.; Pulgarin C.; Albers P.; Kiwi J., J. Photochem, Photobiol.A., 2003, 161, 27.
- [7] Empedocles; Neuhauser R.; Shimizu K.; Bawendi M.G., Adv. Mater., 1999, 11, 1243.
- [8] Link S.; El-Sayed , Int Rev. Phys. Chem., 2000, 19, 409.
- [9] Andersen P.C.; Rowlen K.L., Appl. Spectroscop., 2002, 56, 124 A.
- [10] Henglein A., Chem. Rev. 1989, 89, 1861.
- [11] Kim S.H.; Ribeiro G.M.; Ohlberg D.A.A.; Williams R.S., Heath J.R., J.Phys. Chem., 1999, 103, 10341.
- [12] Zuhuang J., Bactericidal nanosilver cloth and its making proces and use. Patent number CN 1387700, 2003.
- [13] Chen C.M.S., Process for preparing antibacterial antimildew polyacrylic fibers and its filter net for air condyioner. Patent number CN 1355335, 2003.
- [14] Lee H.J.; Yeo .S.Y.; Jeong, J. Mat. Sci., 2003,38, 2199.
- [15] Balasubramanian K., J. Phys. Chem., 1989, 93, 6585.
- [16] Ichihara K.T.; Fujita Y.; Matsuo T., Sakuray T.; Matsuda H., Int. J. Mass, Spectrom. In. Proc., 1985, 67, 229; ibid. 1986, 74, 33.
- [17] Handschuh H.; Cha C.Y.; Bechthold P.S.; Ganteför, Eberhatdt W., J. Chem. Phys., 1995, 102, 6406.

- [18] Haslett T.L.; Bosnick K.A.; Fedrigo S.; Moskovits M., *J. Chem.* 1999, 11, 14, 6456.
- [19] Wedum E.E.; Grant E.R.; Cheng P.Y.; Willy K.F.; Duncan M.A., *J. Chem. Phys. Lett.*, 1991, 100, 6312.
- [20] Félix C.; Sieber C.; Harbich W.; Buttet J.; Rabin I.; Schultze W. Ertl, *Chem. Phys. Lett.*, 1999, 313, 195.
- [21] Howard J.A.; Sutcliffe R.; Mile B., *Surf. Sci.*, 1985, 156, 214.
- [22] Haslett T.L.; Bosnick K.A.; Moskovits M., *J. Chem. Phys.*, 1998, 108, 3453.
- [23] Rabin I.; Jackschath C.; Schultze W., *Z. Phys. D*, 1991, 19, 153. Jackschath, Rabin I.; Schultze W., *ibid*, 1992, 22, 517.
- [24] Allameddin G.; Hunter J., Cameron D.; Kappes M.M., *Chem. Phys. Lett*, 1992, 192, 122.
- [25] Ho J.; Ervin K.M.; Lineberger, *J. Chem. Phys.* 1990, 93, 6987.
- [26] Leopold, D.G.; Ho J.; Lineberger W.C., *J. Chem. Phys.*, 1987, 86, 1715.
- [27] Taylor K.J., Pettiette-Hall C.L.; Cheshnovsky O.; Smalley, *J. Chem. Phys.*, 1992, 96, 3319.
- [28] Handuschu H.; Chaa C. Y.; Bechtold P.S., Ganteför G.; Eberhatdt, *J. Chem. Phys.*, 1995, 102, 6406.
- [29] Okazaki T.; Saito Y., Kasuya A., Nishina Y., *J. Chem. Phys.*, 1996, 104, 812.
- [30] Tiggesbäumker T.; Köller L., Meiwes-Broer K.; Liebesch A., *Phys. Rev. A*, 1993, 48, 1749.
- [31] Minemoto, Iseda M., Kondow T., *Eur. Phys. J.D.*, 1999, 9, 163.
- [32] Bonačić Koutecký V.; Češpiva; Fantucci P.; Pittner J.; Koutecký J., *J. Chem. Phys.*, 1994, 100, 1.
- [33] Santamaria R.; Kaplan I. G.; Novaro O.; *Chem. Phys. Letters*, 1994, 218, 395.
- [34] Liu Z.F.; Yim W.L.; Tse J.S.; Hafner J., *Eur. Phys. J.D.*, 2000, 10, 105.
- [35] Zhao J.; Luo Y.; Wang *Eur. Phys., J. D*, 2001, 14, 309.
- [36] Legge Sue F., Nyberg Graeme L., Peel Barrie J., *J. Phys. Chem A*, 2001, 105, 7905.
- [37] Weis P.; Bierweiler T.; Gilb S.; Kappes M.M., *Chem Phys. Lett.*, 2002, 355, 355.
- [38] Mitrić, Hartmann M.; Stanca B.; Bonačić Koutecký V.; Fantucci, *J. Phys. Chem.*, 2001, A 105, 8892.
- [39] Poteau R.; Heully J.L.; Spiegelman F.; *Z. Phys. D*, 1997, 49, 479.
- [40] Tian Z.M., Tian Y.; Wei W.M.; He T.J.; Chen D.M.; Liu F.C., *Chem. Phys. Lett*, 2006, 420, 450.
- [41] Wedum E.E., Grant E.R., Chang P.Y.; Willey K.F.; Duncan M.A., *J. Chem. Phys.*, 1994, 100.
- [42] Cheng P.Y.; Duncan M.A., *Chem Phys. Lett.*, 1988, 152, 341.
- [43] Ellis M.; Robles E.S.J., Millar I.A., *Chem Phys. Letter.*, 1993, 201 132.
- [44] Bonačić Koutecký V.; Veyeret V.; Mitric R., *J. Chem. Phys.*, 2001, 115, 10450.
- [45] Hay P.J.; Wadt W.R., *J. Chem. Phys.*, 1985, 82, 284.
- [46] Hay P.J.; Wadt W.R., *J. Chem. Phys.*, 1985, 82, 299.
- [47] Boo D. Wan; Ozaki Y.; Andersen L. H.; Lineberger W.C., *J. Phys. Chem A.*, 1997, 101, 6688.
- [48] Ho J.; Ervin K.M., Lienberger W.C., *J. Chem. Phys.* 1990, 93, 6987.
- [49] Bagatur'yants A.A.; Safanov A.A., Stoll H.; Werner H.J., *J. Chem. Phys.*, 1998, 109, 3096.
- [50] Boo Wan D., Ozaki Y., Andersen L. H.; Lineberger W.C., *J. Phys. Chem A.*, 1997, 101, 6688.
- [51] Schultze W.; Becker H.U.; Minkwitz R.; Mansel K., *Chem. Phys. Letters*, 1978, 55, 59.
- [52] Moskowits M., DiLella D.P., *J. Chem. Phys.*, 1980, 72, 2267.
- [53] Joward J.A.; Preston K.F.; *J. Am. Chem. Soc.* 1981, 103, 6226.
- [54] Kernisant K., Thompson G.A., Lindsay D.M., *J. Chem. Phys.*, 1985, 82, 4739.
- [55] Morse M.D., *Chem. Rev.* 1986, 86, 1049.
- [56] Bonačić-Koutecký V.; Češpiva L., *J. Chem. Phys.*, 1993, 98, 7981.
- [57] Basch H., *J. Am. Chem. Soc.*, 1981, 103, 4657.
- [58] Matulis V.E.; Ivashkevich O.A.; Gurin V.S., *J. Molec. Struct. (Theochem)*, 2003, 664-665, 291.
- [59] Häkkinen H.; Moseler M.; Landman Uzi, *Physical Rev. Lett.*, 2002, 89, 033401-1.
- [60] Huda M.N.; Ray A.K., *Eur. Phys. J. D*, 2003, 22, 217.
- [61] Boo Wan D.; Ozaki Y., Andersen L. H.; Lineberger W.C., *J. Phys. Chem A.*, 1997, 101, 6688.
- [62] Spasov V.A., Lee T.H.; Maberry J.P.; Ervin K.M., *J. Chem. Phys.*, 1999, 110, 5208.
- [63] Shi Y., Spasov V.A., Ervin K.M., *J. Chem. Phys.*, 1999, 111, 938.
- [64] Moore C.E., Atomic energy levels, NSRDS-NBS Circular No. 467, USGPO, Washington, 1949.
- [65] Zuhuang J., Bactericidal nano-silver cloth and its making process and use. Patent number CN 1387700, 2003.
- [66] Rabin I., Jackschath C.; Schulze W., *Z. Phys. D*, 1991, 19, 153., Jackschath C., Rabin I.; Schulze W., *ibid*, 1992, 22, 517.
- [67] Ekardt W., *Phys. Rev. B*, 1984, 29, 1558.
- [68] C.E. Moore, Atomic energy levels, NSRDS-NBS Circular No. 467, USGPO, Washington, 1949.
- [69] Foresman J.B., Frisch A., Gaussian, Inc. Pittsburgh, PA, 230-249, 1996.
- [70] I. Rabin, W. Schultze, G. Ertl, *Chemical Physics Letters*, 312, 394-398, 1999.
- [71] I. Rabin, W. Schulze, G. Ertl, C. Felix, C. Sieber, W. Harbich, J. Buttet, *Chemical Physics Letters*, 320, 59-64, 2000.

- [72] E.C. Cosgriff, C.T. Chantler, C. Witte, L.F. Smale, C.Q. Tran, *Physics Letters A*, 343, 174-180, 2005.
- [73] S. Fedrigo, W. Harbich, and J. Buttet, *Physical Review B*, 47(16), 10706-10715, 1993.
- [74] George Alameddin, Joanna Hunter, Douglas Cameron and Manfred M. Kappes, *Chemical Physics Letters*, 192(1), 123-128, 1992.
- [75] H. Handschuh, Chia-Yen Cha, P. S. Bechthold, G. Ganteför, and W. Eberhardt, *J.Chem. Phys.*, 102(16), 6406-6422, 1995.
- [76] I. Katakuse, T. Ichijara, *International Journal of Mass Spectrometry and Ion Processes*, 74, 33-41, 1986.
- [77] W. Schulze, H. Becker, R. Minikwitz, K. Manzel, *Chemical Physics Letters*, 55 (1), 59-61, 1978.
- [78] Joe Ho, Kent M. Ervin, W.C. Lineberger, *J. Chem. Phys.*, 93 (10), 6987-7002, 1990.
- [79] G. V. Krylova, A. M. Eremenko, N. P. Smirnova, S. Eustis, *Theoretical and Experimental Chemistry*, 41 (2), 2005.
- [80] M.Virginia Popa, *International Journal of Computational and Theoretical Chemistry online*, 2 (6), 46-68.